

Functionalized Calix[8]arenes, Synthesis and Self-assembly on Graphite

Jian Zhang,[†] Ganna Podoprygorina,[‡] Vasiliy Brusko,^{‡,§} Volker Böhmer,^{*,‡} and Andreas Janshoff^{*,†}

Institut für Physikalische Chemie, Fachbereich Chemie und Pharmazie, Johannes Gutenberg-Universität, Welderweg 11, D-55099 Mainz, Germany, and Abteilung Lehramt Chemie, Fachbereich Chemie und Pharmazie, Johannes Gutenberg-Universität, Duesbergweg 10–14, D-55099 Mainz, Germany

Received November 18, 2004. Revised Manuscript Received March 3, 2005

With the intention of building hollow tubular structures by self-assembly, we have designed and successfully synthesized a series of calix[8]arene derivatives. Their phenolic units were functionalized in *p*-position by various groups which are able to interact via hydrogen bonding or π – π stacking. Ethynyl, amide, urea, or imide links were chosen for the covalent attachment of these functional groups, to ensure the adjustment of an optimal distance for their interaction. Two different kinds of nanostructures self-assembled on a highly oriented pyrolytic graphite (HOPG) surface were found by scanning force microscopy: parallel aligned nanorods in which the calixarene molecules are adsorbed edge-on on the graphite, providing evidence that these calix[8]arene derivatives stack in a tubular fashion, and micrometer long fiber bundles most probably composed of many nanorods.

Introduction

One-dimensional (1D) structures with lateral dimensions in the range of several to several hundred nanometers have received the focus of intensive research due to their peculiar properties and their potential applications in mesoscopic physics and for the fabrication of nanoscale devices.¹ In recent years, a variety of chemical methods have been used to generate such nanostructures by the so-called “bottom-up” approach. The organization of suitable building blocks via reversible bonds has several advantages over covalent syntheses, and organic tubular self-assemblies may be mentioned as attractive examples.²

Calixarenes represent a class of macrocyclic oligomers which not only are available in larger quantities by simple one-pot syntheses but also can be chemically modified in numerous ways by reactions involving the narrow and/or the wide rim.^{3–5} Additionally calix[4]arenes may be fixed in certain conformations, and examples for the self-organization

of calix[4]arenes reach from dimeric capsules in solution,^{6–8} in which two cone conformers are held together by hydrogen bonds to coordination polymers in the crystalline state built up by the 1,3-alternate conformer.⁹ The rigid skeleton of the cone conformer has proved fruitful also in the synthesis of tubular assemblies, including the *p*-sulfonatocalix[4]arene systems of Atwood et al.¹⁰ and the calix[4]hydroquinones recently studied by Kim et al.^{11,12}

Due to their larger molecular size, calix[8]arenes¹³ are conformationally more flexible than the cone-shaped calix[4]arenes. In their so-called “pleated loop conformation”, stabilized by intramolecular hydrogen bonds, they provide a cavity with an internal diameter of 0.7–0.8 nm, which has

* To whom correspondence should be addressed. E-mail: (A.J.) janshoff@mail.uni-mainz.de; (V.B.) vboehmer@mail.uni-mainz.de.

[†] Institut für Physikalische Chemie.

[‡] Abteilung Lehramt Chemie.

[§] Present address: Chemical Department, Kazan State University, Kremlevskaya St. 18, 420008 Kazan, Russia.

- (1) Xia, Y.; Yang, P.; Sun, Y.; Wu, Y.; Mayers, B.; Gates, B.; Yin, Y.; Kim, F.; Yan, H. *Adv. Mater.* **2003**, *15*, 353.
- (2) (a) Bong, D. T.; Clark, T. D.; Granja, J. R.; Ghadiri, M. R. *Angew. Chem., Int. Ed.* **2001**, *40*, 988. (b) Ohira, A.; Sakata, M.; Taniguchi, I.; Hirayama, C.; Kunitake, M. *J. Am. Chem. Soc.* **2003**, *125*, 5057. (c) Safarowsky, C.; Merz, L.; Rang, A.; Broekmann, P.; Herrmann, B. A.; Schalley, C. A. *Angew. Chem., Int. Ed.* **2004**, *43*, 1291. (d) Wu, J.; Watson, M. D.; Zhang, L.; Wang, Z.; Müllen, K. *J. Am. Chem. Soc.* **2004**, *126*, 177.
- (3) Böhmer, V. *Angew. Chem., Int. Ed. Engl.* **1995**, *34*, 713.
- (4) (a) Gutsche, C. D. *Calixarenes*; Royal Society of Chemistry: Cambridge, U.K., 1989. (b) Gutsche, C. D. *Calixarenes Revisited*; Royal Society of Chemistry: Cambridge, U.K., 1998. (c) Mandolini, L.; Ungaro, R., Eds.; *Calixarenes in Action*; Imperial College Press: London, 2000.

- (5) Asfari, Z.; Böhmer, V.; Harrowfield, J.; Vicens, J., Eds.; *Calixarenes 2001*; Kluwer Academic: Dordrecht, The Netherlands, 2001.
- (6) Rudkevich, D. Self-Assembly in Solution. In *Calixarenes 2001*; Asfari, Z.; Böhmer, V.; Harrowfield, J.; Vicens, J., Eds.; Kluwer Academic: Dordrecht, The Netherlands, 2001.
- (7) (a) Vysotsky, M. O.; Thondorf, I.; Böhmer, V. *Angew. Chem., Int. Ed.* **2000**, *39*, 1264. (b) Vysotsky, M. O.; Thondorf, I.; Böhmer, V. *Chem. Commun.* **2001**, 1890. (c) Thondorf, I.; Broda, F.; Rissanen, K.; Vysotsky, M. O.; Böhmer, V. *J. Chem. Soc., Perkin Trans. 2* **2002**, 1796. (d) Pop, A.; Vysotsky, M. O.; Saadioui, M.; Böhmer, V. *Chem. Commun.* **2003**, 1124.
- (8) (a) Conn, M. M.; Rebek, J., Jr. *Chem. Rev.* **1997**, *97*, 1647. (b) Rebek, J., Jr. *Chem. Commun.* **2000**, 637.
- (9) (a) Mislin, G.; Graf, E.; Hosseini, M. W.; De Cian, A.; Kyrtsakas, N.; Fischer, J. *Chem. Commun.* **1998**, 2545. (b) Akdas, H.; Graf, E.; Hosseini, M. W.; De Cian, A.; Harrowfield, J. McB. *Chem. Commun.* **2000**, 2219.
- (10) Orr, G. W.; Barbour, L. J.; Atwood, J. L. *Science* **1999**, *285*, 1049.
- (11) Hong, B. H.; Bae, S. C.; Lee, C.-W.; Jeong, S.; Kim, K. S. *Science* **2001**, *294*, 348.
- (12) Kim, K. S.; Suh, S. B.; Kim, J. C.; Hong, B. H.; Lee, E. C.; Yun, S.; Tarakeshwar, P.; Lee, J. Y.; Kim, Y.; Ihm, H.; Kim, H. G.; Lee, J. W.; Kim, J. K.; Lee, H. M.; Kim, D.; Cui, C.; Youn, S. J.; Chung, H. Y.; Choi, H. S.; Lee, C.-W.; Cho, S. J.; Jeong, S.; Cho, J.-H. *J. Am. Chem. Soc.* **2002**, *124*, 14268.
- (13) Neri, P.; Consoli, G. M. L.; Cunsolo, F.; Geraci, C.; Piattelli, M. Chemistry of Larger Calix[n]arenes (n = 7, 8, 9). In *Calixarenes 2001*; Asfari, Z.; Böhmer, V.; Harrowfield, J.; Vicens, J., Eds.; Kluwer Academic: Dordrecht, The Netherlands, 2001.

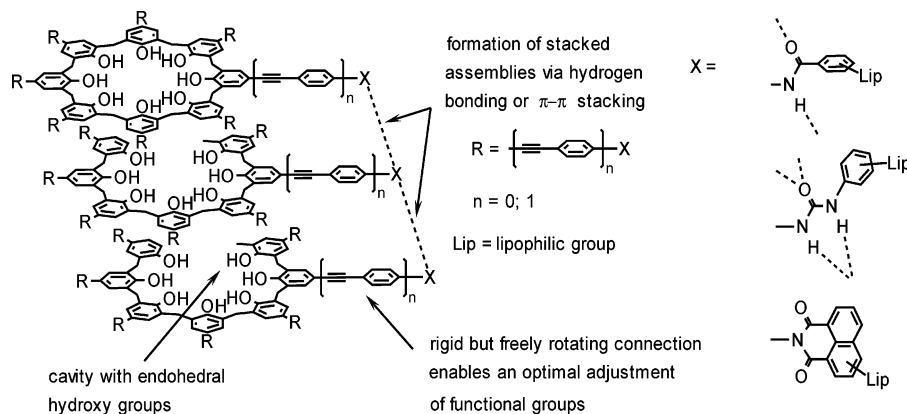


Figure 1. Schematic representation of the possible formation of hollow tubular columns from calix[8]arenes suitably functionalized at the wide rim for self-assembly via intermolecular hydrogen bonding or π - π stacking.

been shown by X-ray crystallography.¹⁴ Additionally, the results from ^1H NMR spectra measured in CDCl_3 revealed a time-averaged D_{4d} symmetry at low temperature; i.e., the conformation found in the crystal structure also exists in solution. As a consequence, it should be conceivable to organize calix[8]arenes into stacked tubular assemblies that could in turn be used as soft templates to include small molecules or metal cations by coordination with “intra-annular” hydroxyl or phenolate groups of the calixarene molecules.^{14,15} Here, we present a thorough study on the assembly behavior of calix[8]arene derivatives designed to form stacked nanotubes. Substituents were introduced in the para-position of the phenolic subunits of calix[8]arenes with the purpose being to modulate their solubility and to create specific interactions between the stacked molecules via hydrogen bonding or π - π stacking (Figure 1). Employing scanning force microscopy (SFM) to visualize the self-assembly of the molecules on highly oriented pyrolytic graphite (HOPG), we found that two types of structures prevail depending on the residues attached to the calixarene molecules: single nanotubes aligned parallel and adjacent to each other and oriented according to the graphite surface and micrometer long nanofibers consisting of bundles showing no specific alignment with graphite.

Experimental Section

Materials. Solvents and all other chemicals were purchased from Acros, Aldrich, and Lancaster and used without further purification. Silica gel (Merck, 0.040–0.063 mm) was used for column chromatography. ^1H and ^{13}C NMR spectra were recorded on a Bruker DRX400 Avance instrument (at 400 and 100 MHz, respectively). FD and ESI mass spectra were measured on a Finnigan MAT 8230 spectrometer and a Micromass Q-TOF Ultima3 instrument, respectively. Melting points are uncorrected. Compounds **I**, **II**, **1**, **2**, **8**, **11**, and **13** were prepared as described.^{16,17}

General Procedure for the Preparation of Octaimidocalix[8]arenes 3–5. The octaamino calix[8]arene octamethyl ether **I** (0.050 g, 0.0462 mmol) and the respective 1,8-naphthalic anhydride (0.462 mmol) were refluxed in dry pyridine (2 mL) in the presence of $\text{Zn}(\text{OAc})_2$ (0.085 g, 0.462 mmol) for 48–72 h. After cooling to

room temperature, the reaction mixture was poured into cold 10% HCl solution (15–20 mL). A thin brown precipitate was filtered off and washed with water (2×20 mL) and methanol (2×20 mL).

Synthesis of Calix[8]arene 3. Calix[8]arene **3** was prepared from compound **I** (0.050 g, 0.0462 mmol), 3,6-didecyloxy-1,8-naphthalic anhydride (0.236 g, 0.462 mmol), $\text{Zn}(\text{OAc})_2$ (0.085 g, 0.462 mmol), 72 h. The precipitate was dissolved in dichloromethane (2–3 mL) and passed through a column (THF/hexane, 1:5, followed by THF) to collect compound **3**. The solvent was removed under reduced pressure, and the residue was triturated with acetone (10 mL), filtered, and washed with acetone (10 mL) to give imide **3** as a light-orange powder. Yield: 0.040 g (17%). Mp: 228 °C. MS (ESI): m/z 5047.72 ($M + \text{Na}^+$), 2534.24 ($M + 2\text{Na}^+$). ^1H NMR ($\text{THF}-d_8$): δ 7.72 (s, Ar-H, 16 H), 7.28 (s, Ar-H, 16 H), 7.06 (s, Ar-H, 16 H), 4.10 (s, Ar-CH₂-Ar, 16 H), 4.00 (m, -O-CH₂-, 32 H), 3.53 (s, -O-CH₃, 24 H), 1.79 (m, -O-CH₂-CH₂-, 32 H), 1.47 (m, -O-(CH₂)₂-CH₂-, 32 H), 1.28 (m, -(CH₂)₆-CH₃, 192 H), 0.86 (m, -CH₃, 48 H).

Synthesis of Calix[8]arene 10. An excess of Et_3N (0.10 mL, 0.712 mmol) was added to a suspension of calix[8]arene **I** (0.020 g, 0.0185 mmol) and *p*-nitrophenylurethane of *p*-decyloxyaniline (0.123 g, 0.296 mmol) in tetrahydrofuran (THF; 5 mL)/CH₂Cl₂ (1 mL). The reaction mixture was refluxed for 5 min and left in an ultrasonic bath at room temperature for 1.5 h. After the reaction was complete, indicated by the formation of a clear solution, methanol (20 mL) was added and the mixture was refluxed for 5 min to form after cooling to room temperature a yellowish precipitate which was filtered off and washed with methanol (3×10 mL) to give pure **10** as a beige powder. Yield: 0.031 g (50%). Mp: >220 °C (decomp.). MS (ESI): m/z 3307.67 ($M + \text{Na}^+$), 1665.20 ($M + 2\text{Na}^+$). ^1H NMR ($\text{DMSO}-d_6$): δ 8.34 (s, -NH-, 8 H), 8.17 (s, -NH-, 8 H), 7.09 (d, Ar-H, 16 H, $^3J_{\text{HH}}$ 6.8 Hz), 6.93 (s, Ar-H, 16 H), 6.63 (d, Ar-H, 16 H, $^3J_{\text{HH}}$ 6.2 Hz), 3.83 (br.s, Ar-CH₂-Ar, -OCH₂-, 32 H), 3.40 (s, -O-CH₃, 24 H), 1.64 (br.s, -O-CH₂-CH₂-, 16 H), 1.35 (br.s, -O-(CH₂)₂-CH₂-, 16 H), 1.23 (br.s, -(CH₂)₇-CH₃, 112 H), 0.84 (br.s, -CH₃, 24 H).

General Procedure for the Preparation of Octaarylethynylcalix[8]arenes. A slurry of octaiodo calix[8]arene octaacetate **II**, arylacetylene (or alkylacetylene in the case of **17**), $(\text{Ph}_3\text{P})_2\text{PdCl}_2$, Ph_3P , and Et_3N or *i*-Pr₂NH in THF was degassed and stirred for 1 h at room temperature. Then CuI was added, and the mixture was degassed again and stirred under N₂ for 48 h at room temperature or refluxed for 72 h.

Synthesis of Calix[8]arene 14. Calix[8]arene **14** was prepared from compound **II** (0.424 g, 0.193 mmol), 4-ethynylbiphenyl (0.419

(14) Gutsche, C. D.; Gutsche, A. E. *J. Inclusion Phenom.* **1985**, *3*, 447.

(15) Bolte, M.; Brusko, V.; Böhmer, V. *Acta Crystallogr.* **2003**, *E59*, o1691–o1693.

(16) Podoprygorina, G.; Zhang, J.; Brusko, V.; Bolte, M.; Janshoff, A.; Böhmer, V. *Org. Lett.* **2003**, *5*, 5071.

(17) Böhmer, V.; Brusko, V.; Rissanen, K. *Synthesis* **2002**, 1898.

g, 2.351 mmol), (Ph₃P)₂PdCl₂ (0.061 g, 0.087 mmol), Ph₃P (0.025 g, 0.095 mmol), *i*-Pr₂NH (5.0 mL, 35.68 mmol), CuI (0.019 g, 0.10 mmol), THF (20 mL). The reaction mixture was filtered, and the solid was washed with water and EtOH. Then it was extracted with hot THF, and the solvent was removed under reduced pressure. The residue was triturated with Et₂O to give **14** as a powder. Yield: 0.060 g (12%). Mp: >400 °C (decomp.). *R*_f = 0.40 (CHCl₃). MS (ESI): *m/z* 2618.02 (M + Na⁺), 1320.47 (M + 2Na⁺). ¹H NMR (DMSO-*d*₆, 100 °C): δ 7.57 (d, Ar-*H*, 16 H, ³*J*_{HH} 7.4 Hz), 7.56 (d, Ar-*H*, 16 H, ³*J*_{HH} 8.2 Hz), 7.47 (d, Ar-*H*, 16 H, ³*J*_{HH} 8.6 Hz), 7.39 (t, Ar-*H*, 16 H, ³*J*_{HH} 7.4 Hz), 7.30 (t, Ar-*H*, 8 H, ³*J*_{HH} 7.4 Hz), 7.22 (s, Ar-*H*, 16 H), 3.64 (s, Ar-CH₂-Ar, 16 H), 2.02 (s, -CH₃, 24 H). ¹³C NMR (DMSO-*d*₆, 100 °C): δ 19.09 (-CH₃), 29.88 (-CH₂-), 88.66 (C≡C), 88.99 (C≡C), 119.88, 120.66, 125.95, 126.13, 127.11, 128.24, 131.25, 131.46, 132.14, 138.71, 139.91, 147.08, 167.24 (C=O).

Synthesis of Calix[8]arene 16. Calix[8]arene **16** was prepared from compound **II** (0.659 g, 0.301 mmol), ethynylpyrene (0.712 g, 3.147 mmol), (Ph₃P)₂PdCl₂ (0.090 g, 0.128 mmol), Ph₃P (0.023 g, 0.088 mmol), Et₃N (0.5 mL, 3.587 mmol), CuI (0.012 g, 0.063 mmol), THF (25 mL), reflux, 72 h. The solvent was evaporated; the residue was washed with hexane and extracted with toluene. Then toluene was removed under reduced pressure, and the residue was reprecipitated from CH₂Cl₂/hexane. Purification by column chromatography (toluene/CHCl₃) finally gave **16** as a powder. Yield: 0.096 g (11%). Mp: 269–272 °C. MS (ESI): *m/z* 3002.28 (M + Na⁺), 1512.56 (M + 2Na⁺). ¹H NMR (CDCl₃, 50 °C): δ 8.40 (s, Ar-*H*, 8 H), 7.60–8.10 (m, Ar-*H*, 64 H), 7.42 (s, Ar-*H*, 16 H), 3.80 (s, Ar-CH₂-Ar, 16 H), 1.99 (s, -CH₃, 24 H). ¹³C NMR (CDCl₃, 50 °C): δ 20.07 (-CH₃), 30.63 (-CH₂-), 89.22 (C≡C), 94.12 (C≡C), 117.30, 121.88, 124.09, 124.22, 124.28, 125.08, 125.34, 125.49, 125.96, 126.96, 128.03, 128.18, 129.42, 132.38, 132.58, 147.99, 168.31 (C=O).

Synthesis of Calix[8]arene 17. Calix[8]arene **17** was prepared from compound **II** (0.550 g, 0.251 mmol), decylacetylene (0.65 mL, 0.50 g, 3.0 mmol), (Ph₃P)₂PdCl₂ (0.074 g, 0.105 mmol), Ph₃P (0.019 g, 0.0724 mmol), *i*-Pr₂NH (2 mL, 1.43 g, 14.2 mmol), THF (20 mL), CuI (0.009 g, 0.045 mmol). The mixture was filtered, the solvent evaporated, and the residue crystallized from THF/MeOH. Purification by column chromatography (EtOAc/hexane, 1/10) gave **17** as dark-brown glass. Yield: 0.313 g (50%). MS (FD): *m/z* 2500.0 (M⁺). ¹H NMR (CDCl₃, 55 °C): δ 6.99 (s, Ar-*H*, 16 H), 3.57 (s, Ar-CH₂-Ar, 16 H), 2.29 (t, -C≡C-CH₂-, 16 H, ³*J*_{H-H} 7.0 Hz), 1.96 (s, -C(O)-CH₃, 24 H), 1.20–1.59 (m, -(CH₂)₇-, 112 H), 0.88 (t, -CH₃, 24 H, ³*J*_{H-H} 6.4 Hz). ¹³C NMR (CDCl₃, 55 °C): δ 14.01, 19.46, 20.09, 22.67, 28.86, 29.11, 29.20, 29.31, 29.56, 29.62, 31.5, 31.93, 79.79, 90.89, 122.36, 132.12, 132.36, 147.17, 168.27.

Synthesis of Calix[8]arene 20. Calix[8]arene **20** was prepared from compound **II** (3.79 g, 1.729 mmol), 4-ethynyl-(*N*-BOC)-aniline (4.521 g, 20.81 mmol), (Ph₃P)₂PdCl₂ (0.485 g, 0.691 mmol), Ph₃P (106 mg, 0.405 mmol), *i*-Pr₂NH (10.5 mL, 75 mmol), CuI (0.063 g, 0.330 mmol), THF (100 mL); reflux, 72 h. After filtration the solvent was evaporated, and the residue was reprecipitated from CH₂Cl₂/THF/MeOH to give **20** as a slightly brown powder. Yield: 1.846 g (37%). Mp: >500 °C. *R*_f = 0.56 (THF/hexane, 1:1). MS (ESI): *m/z* 2930.53 (M + Na⁺), 1476.69 (M + 2Na⁺). ¹H NMR (CDCl₃, 55 °C): δ 7.34 (d, Ar-*H*, 16 H, ³*J*_{HH} 8.6 Hz), 7.27 (d, Ar-*H*, 16 H, ³*J*_{HH} 8.6 Hz), 6.47 (s, -NH-, 8 H), 7.10 (br.s, Ar-*H*, 16 H), 3.65 (br.s, Ar-CH₂-Ar, 16 H), 1.97 (br.s, -C(O)-CH₃, 24 H), 1.51 (s, -CH₃, 72 H). ¹³C NMR (CDCl₃, 55 °C): δ 20.14, 28.37, 32, 80.88, 87.95 (C≡C), 88.79 (C≡C), 117.48, 121.76, 118.23, 132.49, 132.33, 138.65, 147.80, 152.38, 168.43.

Synthesis of Calix[8]arene 22. Calix[8]arene **22** was prepared from compound **II** (0.500 g, 0.228 mmol), *N*-(4-ethynylphenyl)-3,4,5-tridecyloxybenzamide (1.968 g, 2.85 mmol), (Ph₃P)₂PdCl₂ (0.067 g, 0.095 mmol), Ph₃P (0.014 g, 0.053 mmol), Et₃N (5.0 mL, 36 mmol), CuI (0.05 g, 0.026 mmol), THF (10 mL). After filtration the solvent was evaporated and the residue was reprecipitated from THF/MeOH, THF/hexane and CH₂Cl₂/MeOH. Flash chromatography (cyclohexane) finally gave **22** as a powder. Yield: 1.283 g (84%). Mp: 168–173 °C. ¹H NMR (THF-*d*₈): δ 9.37 (s, -NH-, 8 H), 7.75 (d, Ar-*H*, 16 H, ³*J*_{HH} 8.1 Hz), 7.41 (d, Ar-*H*, 16 H, ³*J*_{HH} 7.4 Hz), 7.21 (br.s, Ar-*H*, 32 H), 4.00 (br.s, -O-CH₂-, 48 H), 3.72 (br.s, Ar-CH₂-Ar, 16 H), 2.07 (br.s, -C(O)-CH₃, 24 H), 1.02–1.89 (m, -(CH₂)₇-CH₃, 336 H), 0.89 (br.s, -CH₃, 24 H). ¹³C NMR (acetone-*d*₆, 50 °C): δ 14.39, 20.68, 23.40, 27.05, 31.34, 32.74, 70.11, 73.91, 88.94 (C≡C), 90.73 (C≡C), 107.63, 118.82, 121.04, 122.38, 130.69, 132.96, 134.08, 140.59, 142.64, 148.85, 154.02, 166.09, 169.10.

Synthesis of Calix[8]arene 23. A mixture of **22** (0.103 g, 15.4 μmol), K₂CO₃ (0.023 g, 166 mmol), and EtOH (2.0 mL) in THF (2.0 mL) was stirred under reflux for 24 h. Then water and CH₂Cl₂ were added, and the organic phase was separated, washed with water, and dried (MgSO₄). The solvent was evaporated, and the residue was purified by column chromatography (EtOAc/hexane, 1/10) to give **23** as a powder. Yield: 0.040 g (41%). Mp: >450 °C (decomp.). ¹H NMR (CDCl₃: DMSO-*d*₆, 5:2, v/v, 55 °C): δ 9.74 (s, -NH-, 8 H), 7.70 (d, Ar-*H*, 16 H, ³*J*_{HH} 8.8 Hz), 7.37 (d, Ar-*H*, 16 H, ³*J*_{HH} 8.8 Hz), 7.17 (s, Ar-*H*, 16 H), 7.15 (s, Ar-*H*, 16 H), 3.77–4.07 (m, Ar-CH₂-Ar, -O-CH₂-, 64 H), 1.54–1.81 (m, -O-CH₂-CH₂-, 48 H), 1.02–1.50 (m, -(CH₂)₆-CH₃, 288 H), 0.81 (br.s, -CH₃, 24 H).

Analytical data for further derivatives not studied by SFM are reported in the Supporting Information.

Scanning Force Microscopy. Submonolayers of calix[8]arene derivatives were prepared by spin-coating. A drop (ca. 10 μL) of solution was deposited on a freshly cleaved HOPG surface (highly oriented pyrolytic graphite, purchased from Plano GmbH, Wetzlar, Germany), and the sample was spun at 1000 rpm for 30 s. Calix[8]arene derivatives were dissolved in dichloromethane, tetrahydrofuran, or chloroform resulting at a concentration between 10⁻³ and 10⁻⁶ mg mL⁻¹.

Samples were imaged at room temperature with a commercial SFM (Nanoscope IIIa, Digital Instruments, Santa Barbara, CA), employing TappingMode using rectangular silicon cantilevers (Nanosensors, 125 μm long, 30 μm wide, 4 μm thick) with an integrated tip, a nominal spring constant of 42 N m⁻¹, and a resonance frequency of 330 kHz. To control and enhance the range of the attractive interaction regime, the instrument was equipped with a special active feedback circuit, called Q-control (Nanoanalytics, Germany) as described previously.¹⁸ The quality factor *Q* of this oscillating system is increased by one order of magnitude. As a consequence, the sensitivity and lateral resolution are enhanced, allowing us to prevent the onset of intermittent repulsive contact and thereby to operate the SFM constantly in the attractive interaction regime. All images shown here display the topography of the sample.

Results and Discussion

Synthesis and Characterization. Synthetic pathways to calix[8]arene derivatives are illustrated in Figure 2. Two strategies were developed to achieve an appropriate connection of functional groups to the calixarene skeleton. The first

(18) Anczykowski, B.; Cleveland, J. P.; Krüger, D.; Elings, V.; Fuchs, H. *Appl. Phys. A* **1998**, *66*, S885.

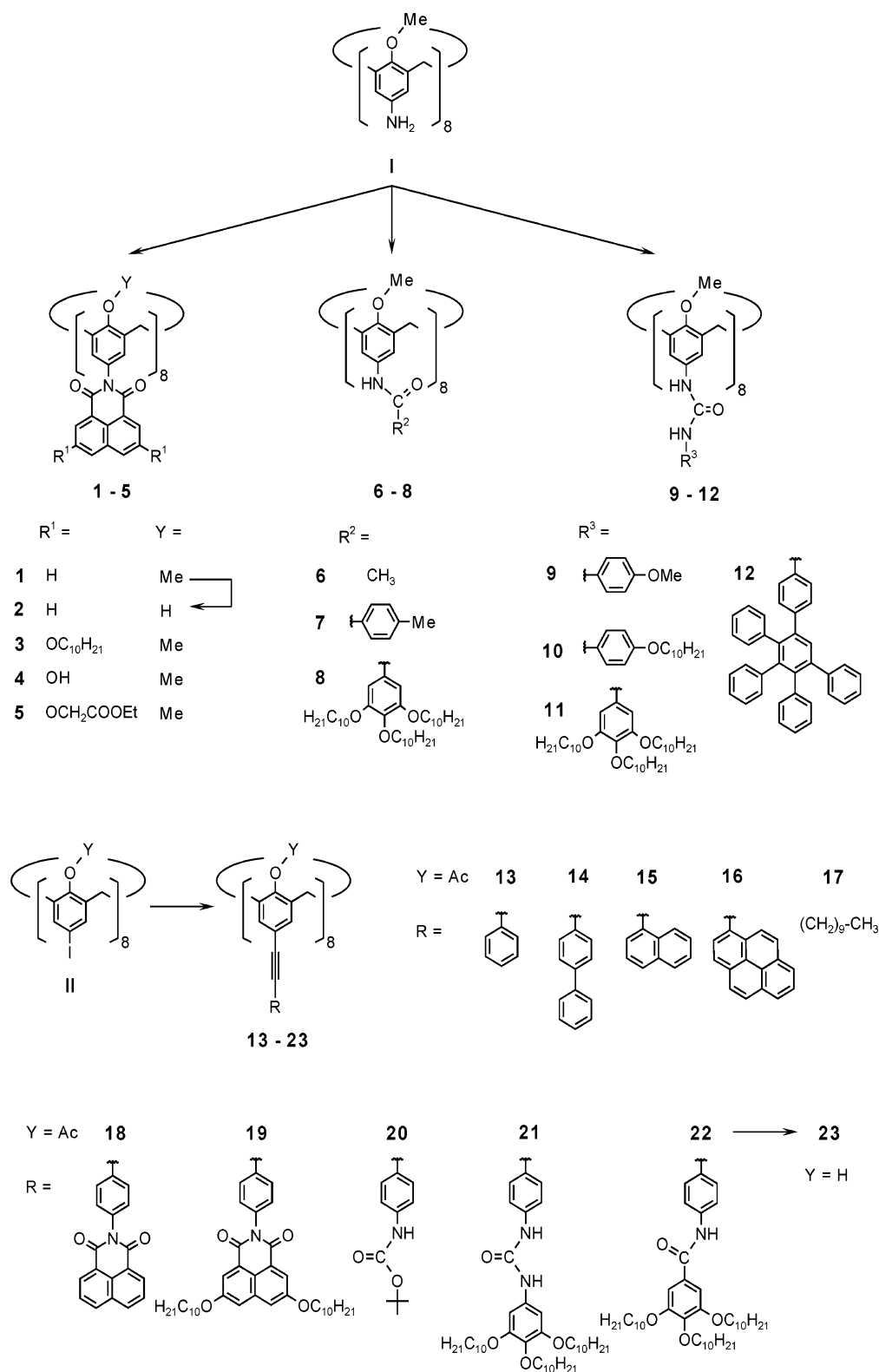


Figure 2. Survey on the calix[8]arene derivatives and their synthesis.

approach is based on the octaamino octamethyl ether **I** which was obtained by exhaustive methylation of *tert*-butyl calix[8]arene (96%), followed by *ipso*-nitration (50–55%) and reduction (60%).¹⁶

The amino calixarene was converted to octaimides **1**, **3**, **4**, and **5** by reaction with the corresponding 1,8-naphthyl anhydrides (25% excess) in pyridine (110–125 °C, 72 h) using $Zn(OAc)_2$ or $(i\text{-}Pr)_2NEt$ as catalyst. Attempts to acylate

the octaamine in pyridine without a catalyst (pyridine, 120 °C) or with an excess of triethylamine in toluene led only to partially substituted products.

The yield of the octaimide depends remarkably on the size of the substituents in 3,6-positions of the naphthyl units. It is lower for imides **3** (17%) and **5** (18%), disubstituted by bulky groups ($R^1 = OC_{10}H_{21}$, OCH_2COOEt), than for compounds **1** (75%) and **4** (87%) with smaller substituents

($R^1 = H, OH$). Most probably with an increasing degree of acylation the approach of the acylating reagent to the unreacted amino groups is sterically more and more hindered. The imide **2** was easily obtained in 90% yield from imide **1** by cleavage of the methoxy groups with BBr_3 (CH_2Cl_2 , -70 °C to room temperature).

The room-temperature 1H NMR spectra of imides **3** ($THF-d_8$), **4** ($DMSO-d_6$), and **5** ($CDCl_3$) show sharp singlets for methylene bridges, for the methoxy groups, and for the aromatic protons of the calix[8]arene. Due to their poor solubility (especially of **2**) the 1H NMR spectra of imides **1** and **2** were measured in $DMSO-d_6$ at higher temperature (75 °C) to confirm the absence of methoxy groups in imide **2**.

Acylation of the octaamino calix[8]arene with acid chlorides (or anhydrides) in the presence of Et_3N at room temperature (12 h) leads to amides **6–8** in 51–90%. The structure and purity of amides **6** and **7** were confirmed by 1H NMR spectra at room temperature in $DMSO-d_6$, but their poor solubility in apolar solvents prevented further studies. To increase the solubility the octamide **8** from gallic acid tris-decyl ether was prepared. It shows a clear 1H NMR spectrum in $THF-d_8$, but significant broadening of signals in $CDCl_3$ at room temperature indicates the formation of larger assemblies via hydrogen bonding between amide units.

The octaureas **9–12** were easily prepared in 50–66% yield by reaction of octamine **1** with an appropriate isocyanate or (*p*-nitrophenyl)urethane at room temperature. Very broad signals in the 1H NMR spectra in $CDCl_3$, CD_2Cl_2 , and $THF-d_8$ at room temperature suggest again that an association of the molecules takes place in solution due to hydrogen bonding ($CDCl_3$, CD_2Cl_2) or π – π -stacking of aryl units (THF). Clear 1H NMR spectra were observed only in $DMSO-d_6$. In case of compounds **9**, **11**, and **12** higher temperature (120–130 °C) was required to dissolve the compounds for the measurements and/or to obtain a better resolution of the signals.

The second strategy was based on the Sonogashira cross-coupling of the octaiodo derivative which was prepared from *tert*-butylcalix[8]arene by *trans*-butylation (93%), followed by iodination (73%) and acylation (92%).¹⁷ Cross-coupling of the octaiodocalix[8]arene with the respective arylacetylene (alkylacetylene) under standard conditions in THF gave the ethynyl derivatives **13–22** in 9–84% yields. A decrease of the yield is observed for coupling reactions with ethynylbiphenyl, 1-ethynyl-naphthalene, and bulky ethynylpyrene **14–16** (9–12%) and also for octaurea **21** (18%). This could be explained by steric hindrance in the cases of **15** and **16** and low stability in the case of **21**. Compound **23** was synthesized by hydrolysis of the octaacetate **22** under alkaline conditions (K_2CO_3 , reflux in $EtOH/THF$) in 41% yield.

In addition to 1H NMR all compounds were confirmed by FD or ESI mass spectra.

Nanostructures Formed by Calix[8]arene Derivatives.

A representative selection of 11 compounds out of a total of 23 synthesized calix[8]arene derivatives (Figure 2) were deposited on graphite and investigated by SFM. In the following section we focus on the self-organization of the components **8**, **13**, **16**, **20**, **22**, and **23** since they exhibit increased solubility and carry para-substituents that are

capable of establishing different intermolecular interactions such as π – π stacking or hydrogen bonds.

Figure 3A shows a SFM image of the calix[8]arene derivative **8** deposited on HOPG employing noncontact mode using enhanced Q -values rendering the imaging procedure less destructive and increasing the lateral resolution by roughly 30%.¹⁸ The molecules are highly organized in cylindrical structures composed of individual calix[8]arenes, which may be named “nanotubes” or “nanorods”. The graphite surface is highly covered with domains of parallel-aligned nanotubes exhibiting a mean spacing of 5.2 ± 0.5 nm between the individual nanotubes. The average width of the domains is about 50 nm, while the length of the nanotubes varies between 50 and 500 nm up to 1.5 μm in rare cases. The height of these structures is about 1 nm, indicating that the nanotubes consist of single calix[8]arenes stacked in a row of coins fashion as schematically illustrated in Figure 4A.

This interpretation is supported not only by the fact that rod formation cannot be explained by calixarene monomers adsorbed with the ring opening perpendicular to the surface since there is no preferred assembly route in this case but also by the finding that it was impossible to resolve the substructure of the nanorods by either SFM or STM. Typical images of calix[8]arenes oriented with the ring opening perpendicular to the surface can be found in a recent publication of Bai et al.¹⁹

The self-assembled nanotubes were stable and could be imaged by SFM for several hours. From the orientation of the domains, which are either oriented parallel (0°) or at an angle of 60 or 120° with respect to each other, we conclude that the underlying graphite with its hexagonal structure governs the assembly of the nanotubes. It is conceivable that the alkyl chains of **8** contribute considerably to the interaction of the molecules with the graphite lattice. However, Figure 3B shows that **13** exhibits essentially the same structure, leading to the assumption that the phenyl group governs the assembly route in this particular case.

Spin coating of dilute solutions of calix[8]arene derivative **16** results in two different superstructures on HOPG. Single long nanofibers were found at high calixarene concentration ($\geq 10^{-3}$ mg mL^{-1}). The length of these nanofibers, which are not aligned with respect to the graphite lattice, ranges from several hundred nanometers to several micrometers, while their height elevates to 7 nm in the center (Figure 3C). Presumably they are composed of bundles of individual nanotubes, as illustrated in Figure 4B. This could explain also that the width and height of the fibers decrease from the middle to both ends although no discrete steps could be resolved by SFM. The formation of these long fibers depends sensitively on the concentration of the solution. In contrast to the formation of nanofibers, regions of parallel-aligned nanorods with dimensions similar to those of derivatives **8** and **13** (Figure 3D) were found when the concentration of **16** was decreased ($\leq 10^{-4}$ mg mL^{-1}).

The self-assembly of calix[8]arene derivatives **20**, **22**, and **23** was investigated under analogous experimental conditions.

(19) Pan, G. B.; Liu, J. M.; Zhang, H. M.; Wan, L. J.; Zheng, Q. Y.; Bai, C. L. *Angew. Chem., Int. Ed.* **2003**, 42, 2747.

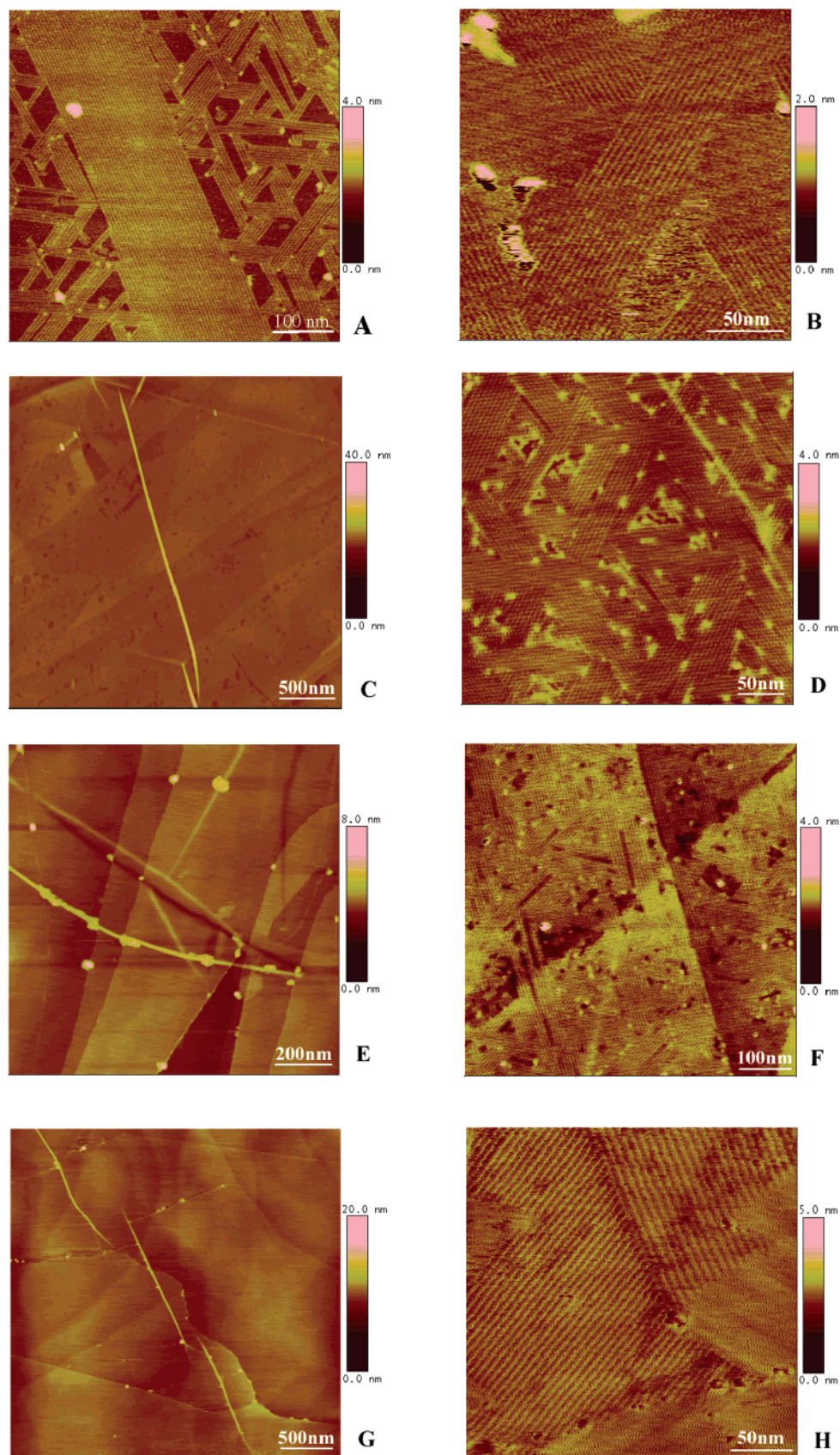


Figure 3. SFM micrographs of various calix[8]arene derivatives spin-coated on HOPG from solution: (A) **8**, CH_2Cl_2 (10^{-4} mg mL^{-1}) see ref 16; (B) **13**, CHCl_3 (10^{-3} mg mL^{-1}); (C) **16**, THF (10^{-3} mg mL^{-1}); (D) **16**, THF (10^{-4} mg mL^{-1}); (E) **20**, THF (10^{-3} mg mL^{-1}); (F) **22**, THF (10^{-3} mg mL^{-1}); (G) **23**, THF (10^{-3} mg mL^{-1}); (H) **23**, THF (10^{-4} mg mL^{-1}).

Parts E–H of Figure 3 show representative SFM images of the nanostructures formed on HOPG. Remarkably, only **16** and **23** show different nanostructures as a function of the

bulk concentration. While at high concentration ($>10^{-3}$ mg mL^{-1}) the formation of disoriented micrometer long nanofibers is favored, parallel-aligned nanorods with a thickness

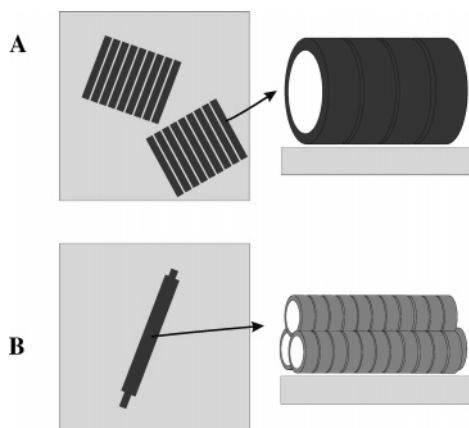


Figure 4. Schematic drawing of the two different assembly schemes: (A) parallel aligned individual nanorods composed of stacked calix[8]arenes attached to the graphite surface edge-on; (B) micrometer long bundles of nanorods.

Table 1. Self-Assembly Behavior of 11 Different Calix[8]arene Derivatives Studied by SFM

sample	solvent	oriented parallel nanorods	disoriented long fibers
3	CH ₂ Cl ₂	×	
8	CH ₂ Cl ₂	×	
10	CH ₂ Cl ₂		×
11	CH ₂ Cl ₂		×
13	CHCl ₃	×	
14	THF	×	
16	THF	×	×
17	THF	×	×
20	THF		×
22	THF	×	
23	THF	×	×

that corresponds to exactly one molecule are observable at low concentration ($\leq 10^{-4}$ mg mL⁻¹). The other four calix[8]arene derivatives (**8**, **13**, **20**, **22**) display only one kind of assembly in the concentration regime up to 10^{-3} mg mL⁻¹. Higher concentration usually results in the deposition of amorphous material. Compound **20** organizes solely in long nanofibers, while parallel-aligned nanorods were exclusively obtained from **8**, **13**, and **22**. Nanofibers that are formed by **23**, **20**, and **16** exhibit heights of 1.5 nm for **23**, 3.5 nm for **20**, and 7.2 nm for **16**. The results are compiled in Table 1, which contains also information about the organization of the compounds **3**, **10**, **11**, **14**, and **17** that are not shown here.

The reason for the different assembly schemes is manifested in the structure of the calixarene derivatives, in particular the residue in the para-position of the phenolic subunits seems to play a key role in the assembly process. In the following section, we will discuss possible scenarios of the nanotube formation. Derivatives **8**, **20**, **22**, and **23** are designed to form *intermolecular hydrogen bonds* between the residues attached to the wide rim of the calixarene molecule with the goal to form hollow nanotubes. Compound **20** has bulky *tert*-butyl residues and hence should exhibit the weakest molecule–molecule as well as molecule–substrate interaction compared with the other three calix[8]arenes that have long alkyl chains. Besides intermolecular hydrogen bonds, **23** is also capable of forming *intramolecular hydrogen bonds* between the hydroxyl groups at the narrow rim. Therefore, **23** may adopt a more flat conformation than the other three derivatives, which might favor the formation of nanotubes by stacking of individual molecules.

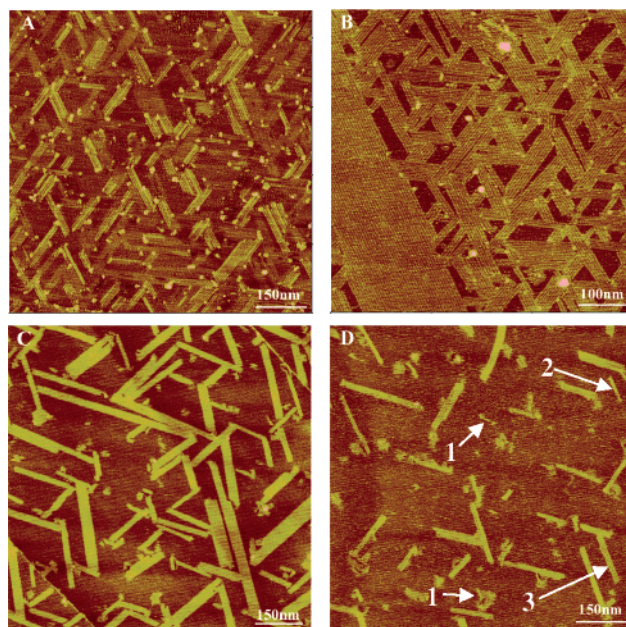


Figure 5. SFM height images of **8** on HOPG prepared by spin coating of solutions with different concentrations in CH₂Cl₂: (A) 10^{-3} , (B) 10^{-4} , (C) 10^{-5} , and (D) 10^{-6} mg mL⁻¹. The height ranging from dark to bright is 5 nm. The surface of A is fully covered with calixarenes, however, only partly displaying nanorods. A decrease of the calixarene concentration results in thinner and shorter domains of nanorods. Single nanorods and assemblies of two or three parallel rods are indicated by arrows.

Compounds **13** and **16** are both designed to form *intermolecular π – π interactions*, but the π – π stacking of **16** bearing pyrene residues is presumably stronger than that of **13** with only phenyl moieties. Both **13** and **16** form parallel aligned nanorods, while **16** also organizes in long nanofibers at higher monomer concentration. It is reasonable to assume that nanofibers are predominately formed, if the intermolecular interaction is stronger than the interaction with the surface, since fewer nucleation sites obviously occur in nanofiber formation than in the case of parallel aligned nanorods. Thus, nanofibers are formed for instance by **16**, **20**, and **23**, which provide strong intermolecular interactions. However, it remains difficult to find a safe relationship between molecular structure and the assembly formed.

In the following section we describe the influence of varying calix[8]arene concentration on the assembly behavior. Of particular interest was the self-assembly of parallel aligned nanorods as a function of monomer concentration. One question we wanted to address is, whether it is possible to visualize individual nanotubes at low concentration.

Figure 5 shows the impact of varying the concentration of **8** on the surface coverage and nanotube formation. We found that decreasing the calixarene concentration of the spin-coating solution results in thinner and shorter nanorod domains. The smaller the domains the more susceptible they are to the scanning procedure as compared to the highly covered surface that is already achieved by using a concentration of 10^{-3} – 10^{-4} mg mL⁻¹.

This leads to the conclusion that lateral interactions between adjacent rods play an important role in the self-organizing process. However, the rods formed from a dilute solution (10^{-5} – 10^{-6} mg mL⁻¹) still show an elongated shape, and sometimes even single nanorods could be found (Figure

5C, D, arrows). This means that an anisotropic cooperativity is observed for the deposition of the molecules from solution since the molecules apparently assemble faster along the direction of the nanorods than in the direction normal to the rods, as strikingly displayed by domains consisting of only two or three nanorods (Figure 5B). This observation supports the assumption that the calixarenes stack due to strong intermolecular interaction once nucleation on the surface occurred.

In conclusion, the formation of nanorods is attributable to the balance of intermolecular interactions and epitaxial effects of the underlying HOPG substrate.

Acknowledgment. These studies were supported by BMBF (03N 6500) in the framework of the Center for Multifunctional Materials and Miniaturized Devices. Financial support by DFG (SFB 625) is also gratefully acknowledged. We warmly thank Prof. Dr. M. U. Schmidt (Johann Wolfgang Goethe-Universität Frankfurt a. M., formerly at Clariant GmbH) for a generous gift of 3,6-dihydroxy-1,8-naphthalic anhydride.

Supporting Information Available: Synthetic procedures and spectral data for compounds not included in the main text (PDF). This information is available free of charge via the Internet at <http://pubs.acs.org>.

CM047980X